All-Aqueous Continuous-Flow RAFT Dispersion Polymerisation for Efficient Preparation of Diblock Copolymer Spheres, Worms and Vesicles†

Sam Parkinson[a], Nicole S. Hondow[a], John S. Conteh, Richard A. Bourne[ab] and Nicholas J. Warren[a]*

We report the scalable, all-aqueous synthesis of poly(dimethyl acrylamide)-poly(diacetone acrylamide) (PDMAm-PDAAm) diblock copolymer spheres, worms and vesicles by reversible addition-fragmentation chain transfer (RAFT) aqueous dispersion polymerisation in a low-cost continuous-flow (CF) reactor. A transient state kinetic profiling method using a 5 mL reactor coil indicated a considerably faster rate than the equivalent batch reaction. Higher throughput was subsequently demonstrated by employing a 20 mL coil reactor for the synthesis of a 135 g, 30 % w/w batch of $PDMAm_{113}$ macromolecular chain transfer agent (macro-CTA) at 98 % conversion. This was used without further purification to polymerise DAAm in a CF reactor. During this polymerisation, the chains underwent polymerisation-induced self-assembly (PISA) producing block copolymer spheres. This reaction also proceeded faster than in batch, and the high resolution kinetics enabled clear observation of the rate enhancement which is characteristic of PISA systems GPC studies indicated the formation of a copolymer with low molar mass dispersity and complete blocking efficiency, despite the high conversion achieved during the precursor macro-CTA synthesis. It was subsequently demonstrated that the $PDMAm_{113}$ macro-CTA could be used to prepare $PDMAm_{113}$-$PDAAm_x$ block copolymer spheres (where x = 50, 100 and 200) with systematically increasing particle diameters. Finally, by reducing the PDMAm macro-CTA DP to 50 and increasing total solids to 20 % w/w , it was possible to prepare worms and vesicles in the tubular reactor by tailoring the residence time to achieve specific degrees of polymerisation of the PDAAm block.

Introduction

Continuous-flow (CF) chemistry has emerged as a key technology in the drive for sustainable and precise chemical synthesis.[1, 2] It is also anticipated that the technology will become a key method for producing novel advanced materials.[3]

Further advances involving integration of sophisticated online monitoring instrumentation into CF synthesis platforms will aid in the development of autonomous, self-learning reactors which are of extreme relevance given the emergence of digital manufacturing technologies.[4-6]

Given that block copolymers are already present in a vast number of advanced materials,[7] precise control of their structure over a variety of scales is of paramount importance. This is easily achieved in batch by using controlled radical polymerisation technologies such as atom transfer radical polymerisation (ATRP),[8] nitroxide mediated polymerisation (NMP)[9] and reversible addition-fragmentation chain transfer (RAFT) polymerisation.[10, 11]

Combining these technologies with continuous flow has been well reported,[12, 13] and was pioneered by Shen and Zhu, who employed CF reactors for synthesis of well-defined polymers and block copolymers via ATRP.[14, 15] Further developments in this area brings about the potential to develop a new generation of complex polymer architectures while the multi-scale nature of CF means that growing demand for the materials can easily be met due to the reduced process research and development required for scale up.

The use of CF reactors for solution RAFT polymerisation followed some time later, but again the reactors proved to be capable of the scalable polymerisation of a wide variety of monomers achieving low molar mass dispersities (Đ). [16, 17] The improved heat transfer and the ability to conduct the reaction at temperatures above the solvent boiling point has also enabled acceleration of the process. [18] CF platforms have more recently been combined with new generation RAFT technologies such as photo-induced RAFT [19-21] and oxygen tolerant PET-RAFT,[22] while novel reactor configurations such as looped flow reactors[23] and the ability to telescope processes has also enabled the preparation multi block copolymers by sequential polymerisation.[24] Using a similar concept, post-polymerisation chemistry such as the removal of the RAFT end-group post synthesis and the use of thiol-ene 'click' chemistry to functionalise polymers is easily achieved[25-27] and modules which enable processes such as degassing, precipitation, dialysis and UV detection[27] can also be integrated into platforms.[28] The precision control has also enabled the synthesis of more complex architectures such as forced gradient[29] polymers, the ability to control the polymer MW distribution[30-32] and the easily tuneable synthesis of highly branched polymers.[33]

Heterogeneous RAFT polymerisation technologies have been widely reported over the last 15 years or so and are popular since they allow rational production of a variety of block copolymer nanoparticles via polymerisation-induced self-assembly (PISA).[34-36] Furthermore, the precise nature enables control not just over the morphology, but the specific dimensions of the resulting nanoparticles.[37, 38]

This precision could provide additional complementary control over polymer nanoparticles within CF systems. Of the relatively few reports where PISA is conducted in tubular reactors, surfactant-free RAFT emulsion polymerisation of methyl methacrylate (MMA),[39] and RAFT dispersion polymerisation of MMA using a poly(poly(ethylene glycol)methyl ether methacrylate in a water/ethanol solvent mixture have both produced well defined spherical particles.[40] There is one recent report of non-spherical morphologies prepared via visible light-mediated PISA in a tubular reactor using a poly(ethylene glycol) macro-CTA.[41] In this work, where only the diblock synthesis was conducted in flow, all three morphologies were produced, but there was a notable loss in polymerisation control when preparing a pure phase of vesicles. Despite precedent for rapid generation of kinetic models using transient kinetic studies,[42-45] the aforementioned studies use steady state kinetic profiling, which, while effective, is both time consuming and uses large volumes of material.

Herein, we construct a low-cost CF reactor which we evaluate for the RAFT aqueous solution polymerisation of dimethylacrylamide (DMAm), and the RAFT aqueous dispersion polymerisation of diacetone acrylamide (DAAm) to produce PDMAm-PDAAm block copolymer nano-objects (see Figure 1a and b). Furthermore, we also apply a transient kinetic profiling technique, and assess whether it is a reasonable alternative to steady state methods.

Batch experiments have previously shown that this copolymer can form nano-objects with predictable morphologies dependent on the degree of polymerisation of the PDAAm block. [46, 47] It therefore provides an extremely convenient proof of concept formulation to evaluate our flow reactor for multi-scale synthesis of block copolymer nano-objects where both macro-CTA and diblock copolymers are synthesised via CF.

Experimental

Materials

4,4'-Azobis(4-cyanovaleric acid) (ACVA, 99%), Dimethyl acrylamide (DMAm, 99%), deuterated methanol (CD_3OD, 99.8%) and deuterium oxide (D_2O, 99.9%) were purchased from Sigma Aldrich (UK). 3-((((1-carboxyethyl)thio)carbonothioyl)thio) propanoic acid (CTTP, 90%) was purchased from Boron Molecular (Raleigh, USA). Diacetone acrylamide (DAAm, 99%) was purchased from Alfa Aesar (UK).

^1H NMR spectra were acquired using a Bruker 500 MHz spectrometer. Samples were dissolved in D_2O or CD_3OD. All chemical shifts are reported in ppm (δ). The average number of scans accumulated per spectrum was typically 32.

Dynamic light scattering measurements were conducted at 25°C using a Malvern Zetasizer Nano series instrument. Light scattering was detected at 173° and hydrodynamic diameters were determined using the Stokes-Einstein equation, which assumes spherical, non-interacting particles.

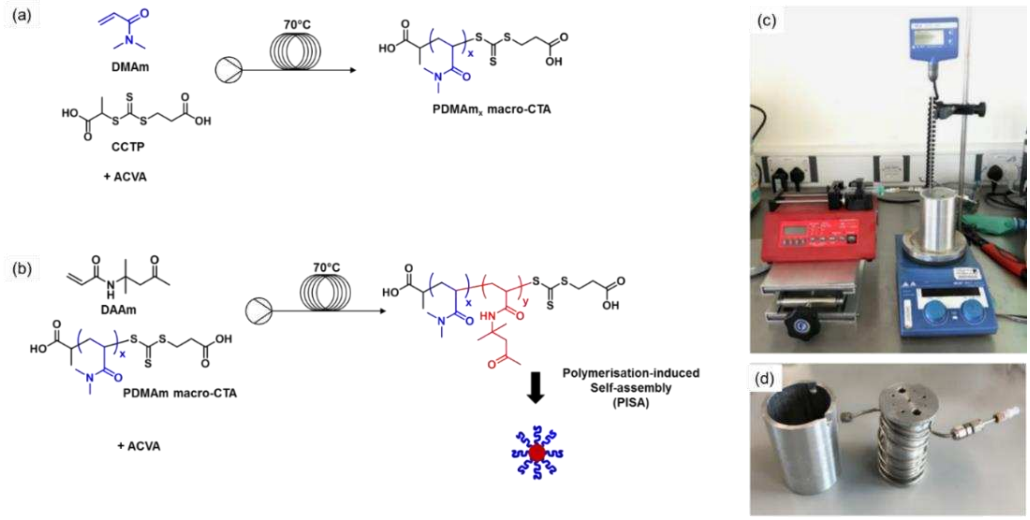

Figure 1. Reaction schemes for the continuous-flow synthesis of (a) Poly (dimethyl acrylamide) [PDMAm] macro-CTA (b) Poly (dimethyl acrylamide) –poly(diacetone acrylamide) [PDMAm-PDAAm] diblock copolymer. (c) Photograph of the continuous-flow configuration (d) Photograph of the dismantled custom built flow-reactor.

Gel permeation chromatography measurements were conducted using an Agilent 1260 Infinity system fitted with two 5 µm Mixed-C columns plus a guard column, a refractive index (RI) detector and an UV/Vis detector operating at 309nm. DMF containing 1.0 % w/v lithium bromide (LiBr) was used as eluent. The pump flow rate was set to 1.0 mL min^{-1} and the temperature of the column oven and RI detector were set to 60 °C. A series of ten near-monodisperse poly(methyl methacrylate) standards (M_p ranging from 800 to 2,200,000 g mol^{-1}) were employed as calibration standards in conjunction with the RI detector for determining molecular weights and molar mass dispersities (*Đ).*

Transmission electron microscopy (TEM) was conducted at 200 kV using a Tecnai F20 FEGTEM. TEM samples were prepared at 0.1 % w/w and stained with a 1 % w/w uranyl acetate solution.

High Resolution Transient Flow Kinetic Studies

A typical protocol for the high resolution transient kinetic profiling experiment was as follows: For $PDMAm_x$ synthesis, DMAm (5 g, 100 eq), CCTP (0.12 g, 1 eq), ACVA (0.01g, 0.1 eq) were added to a round bottom flask and dissolved in H_2O (12 ml) to give a 30 % w/w reaction solution. The flask was, sealed, sparged with nitrogen for 20 minutes. A portion of this reaction solution was then taken up into a 20mL syringe and fitted to a New Era NE-300 syringe pump. The solution was passed through a 5ml, tubular stainless-steel reactor at a flow rate 10 ml min^{-1} for 90 seconds, the flow rate was then reduced to 0.08 ml min^{-1} giving a retention time of 60 minutes. Kinetic samples were collected, in vials, from the reactor outlet changing vials every 144 seconds to give 25 kinetic samples. These samples were then analysed by ^1H NMR and DMF GPC. This protocol was the same for the kinetic experiments conducted on $PDMAm_{113}$-$PDAAm_X$ diblock copolymer syntheses.

Steady State Kinetic Studies

A typical protocol for a batch kinetic study was as follows: For $PDMAm_x$ synthesis, DMAm monomer (20 g, 100 eq), CCTP (0.5 g, 1 eq), ACVA (0.05 g, 0.1 eq) were weighed into to a round bottom flask and dissolved in H_2O (48 mL) to give a 30 % w/w reaction solution. The flask was, sealed, and sparged with nitrogen for 30 minutes. A portion of this reaction solution was then taken up into a 20 mL syringe and fitted to a New Era NE-300 syringe pump. The solution was then pumped through the 5 mL coil at the appropriate flow rate (either 0.5, 0.25, 0.167, 0.125, 0.1 mL min^{-1}). For each flow rate the reactor was allowed to reach steady state by passing through 3 reactor volumes (15 mL) worth of reaction solution. Three samples were then collected from the outlet of the reactor and analysed by ^1H NMR spectroscopy to determine monomer conversion.

Residence Time Distribution Determination

The flow reactor was modified by placing a Rheodyne six-port switching valve (fitted with a 100 µL sample loop) between the pump and the reactor. Deionised water was pumped through the reactor at a flow rate of 1 mL min^{-1} while the switching valve was set to the 'load' position. Under these conditions, the loop was filled with 100 µL of tracer via the loading port (30% % w/w DMAm monomer solution or $PDMAm_{113}$ polymer solution). The switching valve was then moved to the inject position which allowed the tracer solution to enter the reactor noting the exact injection time. The elution of the tracer was monitored using a Knauer K2301 RI detector placed at the reactor outlet.

Batch Kinetics of $PDMAm_x$ mCTA

DMAm monomer (2g, 100eq), CCTP (0.051g, 1 eq), ACVA (0.005g, 0.1 eq) were added to a round bottom flask and dissolved in H_2O (4.8ml) to give a 30 % w/w reaction solution. A stirrer bar was added and then the flask was sealed and sparged with nitrogen for 20 minutes. The sealed flask was then immersed in an oil bath at 70°C and left for 60 minutes. Samples were taken every 5 minutes using a nitrogen purged syringe and analysed by ^1H NMR and GPC.

Batch Synthesis of $PDMAm_x$ mCTA

DMAm monomer (20 g, 100 eq), CTTP (0.51 g, 1 eq), ACVA (0.05 g, 0.1 eq) were added to a round bottom flask and dissolved in H_2O (48 mL) to give a 30 % w/w reaction solution. A stirrer bar was added and then the flask was sealed and sparged with nitrogen for 20 minutes. The sealed flask was then immersed in an oil bath at 70°C and left for 50 minutes. Afterwards the flask was removed from the oil bath and quenched by exposure to oxygen. Samples were taken for ^1H NMR and GPC analysis which indicated 93 % monomer conversion, M_n = 10,700 and $Đ$ =1.09. No further purification was performed and the macro-CTA solution was used as is for further chain extension experiments.

High Throughput Flow Synthesis of $PDMAm_{113}$ mCTA

DMAm monomer (40 g, 100 eq), CTTP (1.02 g, 1 eq), ACVA (0.11 g, 0.1 eq) were added to a round bottom flask and dissolved in H_2O (96 mL) to give a 30 % w/w reaction solution. The flask was sealed and sparged with nitrogen for 20 minutes. A Jasco PU-980 HPLC pump inlet tube was then inserted into the sealed flask and the solution was pumped through a 20 mL stainless-steel tubular reactor which had been equilibrated to 70°C with a retention time of 50 minutes (flow rate = 0.4 mL min^{-1}). The polymer was collected in multiple vials at the reactor outlet. After combining these samples, ^1H NMR and GPC analysis was conducted which indicated > 98% monomer conversion, M_n = 10,300 and $Đ$ = 1.10 . No further purification was performed and the macro-CTA solution was used as is for further chain extension experiments.

Batch kinetics of $PDMAm_{113}$-$PDAAm_X$ copolymer

A typical protocol for the synthesis of $PDMAm_{113}$-$PDAAm_X$ was as follows: DAAm monomer (0.5 g, 50 eq), PDMAm mCTA (0.6 g, 1 eq) and ACVA (0.0016 g, 0.1 eq) were added to a round bottom flask and dissolved in H_2O (9.9 mL) to give a 10 % w/w

reaction solution. A stirrer bar was added and then the flask was sealed and sparged with nitrogen for 20 minutes. The sealed flask was then immersed in an oil bath at 70°C and left for 90 minutes. Samples were taken every 10 minutes using a nitrogen purged syringe for ^{1}H NMR and GPC analysis.

Continuous-Flow Synthesis of PDMAm-PDAAm$_x$ copolymers

A typical protocol for the synthesis of PDMAm-PDAAm$_x$ was as follows: For a target composition of PDMAm$_{113}$-PDAAm$_{50}$, DAAm monomer (1 g, 50 eq), PDMAm mCTA (0.6 g, 1 eq) and ACVA (0.0016 g, 0.1 eq) were added to a round bottom flask and dissolved in H_2O (14.4 mL) to give a 10 % w/w reaction solution. The HPLC pump inlet tube was then inserted into the sealed flask and the solution was pumped through a 5 mL stainless-steel tubular reactor at 70°C with a retention time of 50 minutes (flow rate = 0.1 mL min^{-1}). The polymer was collected in multiple vials at the reactor outlet. Samples were taken from each vial for ^{1}H NMR and GPC analysis to determine when the reactor had reached steady state.

Results and Discussion

Our CF platform comprised either a syringe pump or an HPLC pump connected to a stainless steel tubular reactor (5 mL or 20 mL) coil wrapped around a custom-built aluminium heating block (Figure 1c and d). The total cost of these parts was an order of magnitude cheaper than common commercial flow-reactor systems. This platform was first employed to conduct a kinetic study for the synthesis of the PDMAm macro-CTA using the 5 mL reactor coil. Kinetic profiling for RAFT polymerisation in flow reactors is normally achieved through steady-state sampling, where the reactor is set to a specific residence time, allowed to reach steady state (which can be multiple residence times) and a sample is then collected. This process is repeated for multiple residence times to generate a kinetic plot, requiring large volumes of material and is much more time-consuming than a typical batch kinetic study. An alternative approach is to conduct transient state kinetic sampling. During this process, samples are continuously collected from the reactor but each sample has a different residence time due to specifically controlling pump rates. Under ideal conditions, each sample can be considered to be an individual batch reactor. Various methods for transient kinetic sampling have been reported in the literature for polymer and small-molecule synthesis.[42-45] Based on these literature methods, we developed our own procedure for transient kinetic sampling (Figure 2). The reactor was initially primed using an initial flow-rate of 10 mL min^{-1}

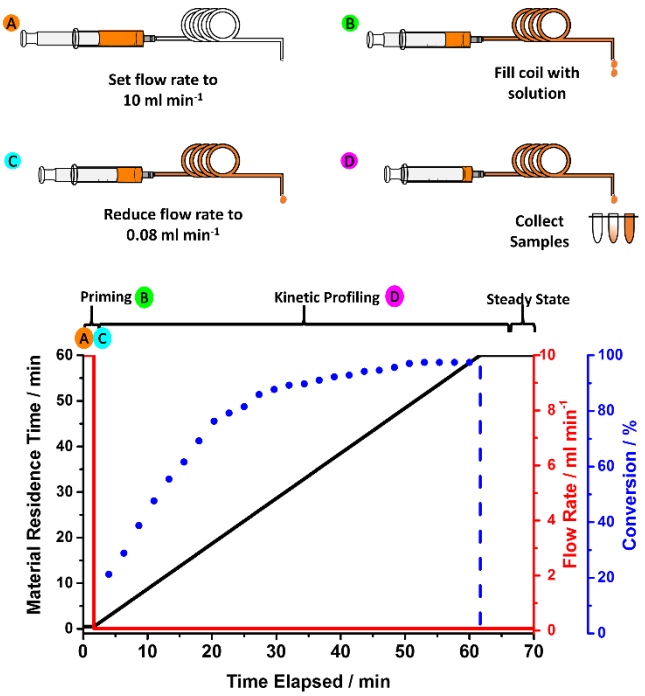

Figure 2. Schematic of high resolution kinetic profiling technique used for monitoring a variety of RAFT polymerisations (A) The pump flow rate is set to 10 mL min^{-1} and pumping is started, (B) The reactor is then primed with reaction solution (C) Once the reactor is filled with solution the flow rate is reduced to give our desired residence time (0.08 mL min^{-1}) (D) Samples are then collected at set intervals from the reactor outlet. Plot indicates material residence time, flow rate and conversion as a function of the experimental time.

until the system reached steady state. This was determined to be approximately 1.5 minutes, beyond which a constant UV response was recorded at the reactor outlet (3 reactor volumes; see Figure S1). The flow rate was then immediately reduced to 0.08 mL min^{-1} and samples were collected from the reactor outlet at regular intervals. These were then characterised by ^{1}H NMR and DMF GPC to determine monomer conversion, molecular weight and molar mass dispersity (*Đ*). These data were compared to an equivalent reaction conducted in batch on a 7 g scale. Although regular kinetic sampling is feasible during rapid batch polymerisation[48, 49], it is more laborious given the need to purge/degas syringes. The monomer conversion was calculated by comparing the integrals from the DMAm vinyl signals between 5.5 ppm and 7.0 ppm to those which result from the overlapping polymer/monomer signals between 2.7 and 3.3 ppm. The data indicated that that > 97 % monomer conversion was achieved during the CF process, which was notably faster than in batch, where only 90 % conversion achieved over the same time period (Figure 3a). This increased rate is more apparent in the steeper gradient observed for CF in the semi-logarithmic rate plots (Figure 3b). Importantly the plots both indicate first-order kinetics (Figure 3b).

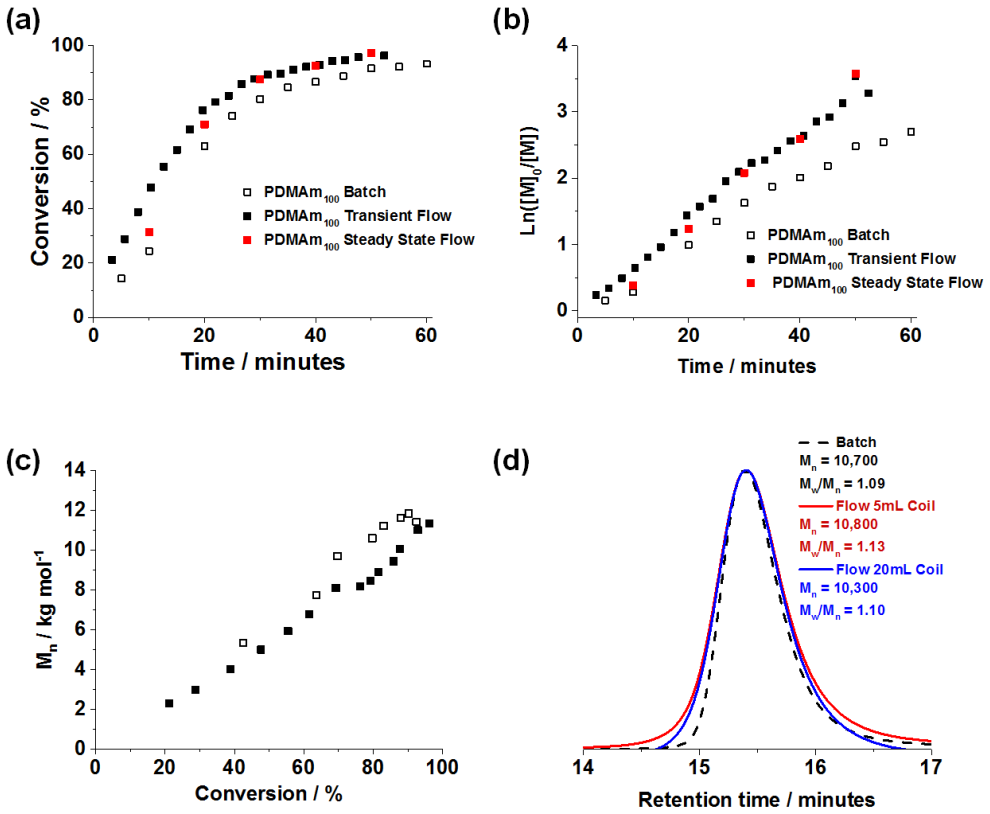

Figure 3. (a) Conversion vs. Time, (b) Semi-logarithmic rate and (c) M_n vs conversion plots for the RAFT aqueous solution polymerisation of dimethyl acrylamide (DMAm) in batch and flow (d) GPC Chromatograms recorded for macro-CTAs synthesised on small scale (batch and flow) and large scale reactor systems (flow only). All reactions were conducted at 70 °C with total solids concentration of 30 % w/w and [DMAm]:[CTA]:[ACVA] = 100:1:0.1.

We also performed steady state flow kinetics at 5 different flow rates. In each case three samples were taken, after 3, 4 and 5 reactor volumes. All samples for a given residence time were judged to have approximately the same conversion, confirming steady state (see Figure S2). The average values for each residence time were superimposable onto the transient data (Figure 3a and b), thus validating our transient kinetic method. The increased rate has been noted previously for other polymerisations in flow[18] and has been attributed to the increased heat transfer under flow conditions. We hypothesise that this phenomenon is amplified during RAFT, which relies on radical decomposition early in the reaction. If this is the case, an increased radical flux would result in a faster polymerisation rate assuming effects of mass transfer in the 2.1 mm O.D. tubing are negligible.[28] One method of achieving efficient heat transfer in batch is to use microwave irradiation, something which has previously shown to produce comparable kinetics.[18] The present work aims to demonstrate the multi-scale capability of our flow reactor, and hence conducting microwave experiments was beyond the scope.

To monitor the molecular weight evolution, kinetic samples were also analysed by gel permeation chromatography (GPC). For both reactions, a linear increase in molecular weight in line with monomer conversion was observed (Figures 3c). Overall, M_n values recorded for the flow polymerisation were subtly lower than the batch equivalent, which can be attributed to the discrepancy in molar mass dispersity ($Đ$; Figure S3), which is equal to M_w/M_n. Nevertheless, the data confirm that CF reactors are able to maintain the pseudo-living behaviour of RAFT polymerisation and produce near equivalent polymers to a batch method for this formulation.

To demonstrate the ability to easily increase product output without significant increase in reactor footprint, we subsequently prepared a relatively large batch of PDMAm macro-CTA. For this, the output was increased by using a 20 mL coil and an HPLC pump set at a flow rate of 0.4 mL min^{-1}, thus providing a residence time of 50 minutes. Approximately 135 g of 30 % w/w polymer solution was obtained and ^{1}H NMR analysis indicated 98 % monomer conversion for this macro-CTA (see spectrum in Figure S4). This conversion is in good agreement with that expected based on the kinetic profile obtained in the smaller flow reactor (Figure 3a).

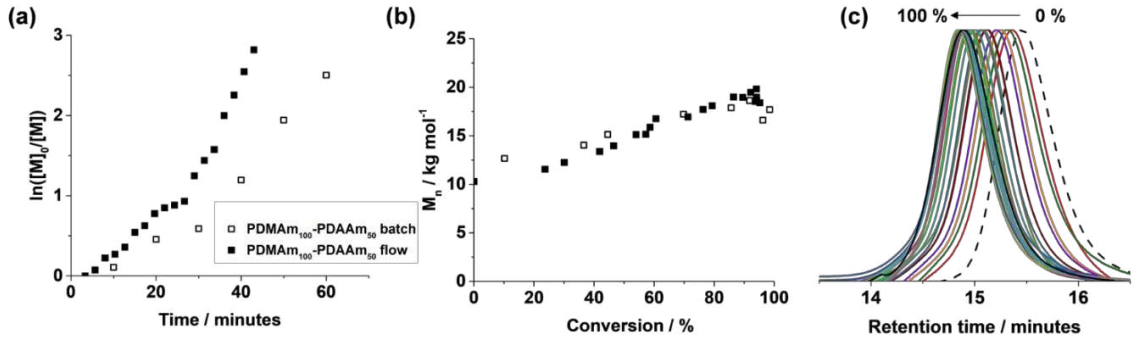

Figure 4. a) Semi-logarithmic rate plots, (b) Mn vs. Conversion for the RAFT aqueous dispersion polymerisation of Diacetone acrylamide using a $PDMAm_{113}$ macro-CTA. (c) Chromatograms obtained for each of the kinetic samples extracted from the reaction conducted using the continuous-flow reactor. For all reactions, total solids concentration of 10 % w/w and [Monomer]:[mCTA]:[ACVA] = 50:1:0.

GPC studies on both batch and flow syntheses of the polymers confirmed comparable molecular weight distributions (see chromatograms in Figure 3d). For the flow synthesis, a number average molecular weight (M_n) of 10,300 was obtained along with a relatively narrow molar mass dispersity (Đ = 1.10). All these parameters corroborated reasonably well with those obtained in an equivalent batch synthesis (M_n = 10,700; $Đ$ = 1.09) but the flow synthesis again produced a polymer with a subtly broader molecular weight distribution. It has previously been reported that polymers synthesised in flow have narrower molar mass dispersity due to improved heat transfer minimising the effects of any exotherm.[50] Here, the differences in dispersity are minimal, suggesting this is not an issue in either the batch or flow. If anything, subtly broader molecular weight distributions should be expected in non-ideal flow reactors due to the residence time distribution observed due to either axial dispersion or laminar flow.[51] These RTDs could also be affected by liquid properties such as viscosity, but in our case, this is not apparent when comparing RTDs for monomer and polymer solutions in the 5 mL reactor (30 % w/w solutions; Figure S5a). However, RTD determination on comparing the 5 mL and 20 mL reactors indicated that the 20 mL coil operated closer to plug flow than the 5 mL coil. This is likely due to any flow interruption, such as dead-zones at connecting joints having more of an influence in the shorter 5 mL reactor. The dispersity observed for the longer batch is indeed lower ($Đ$ = 1.10 for 20 mL coil vs. $Đ$ = 1.13 for 5 mL coil), but it is not clear whether this is small decrease is significant. Nevertheless, the well-defined nature of the macro-CTA produced in each reactor was deemed sufficient, with respect to RAFT polymerisation criteria (high conversion, first order kinetics, linear evolution in M_n with conversion, and $Đ$ < 1.3) for the preparation of block copolymers without further purification.

To evaluate whether it was possible to produce block copolymer nanoparticles using the continuous-flow platform, we repeated the well characterised RAFT aqueous dispersion polymerisation of diacetone acrylamide (DAAm). [46, 47] In the present study, we targeted a PDMAm macro-CTA DP of 100 since it should only form spherical particles at 20 % w/w (actual DP of 113 was calculated after end-group analysis).[46] We anticipated this would minimise potential complications caused by reactor fouling/blockages which are more likely when targeting higher-order morphologies which would change the rheology of the reaction medium.

By once again utilising the convenient sampling method, detailed kinetic studies could also be carried out for this RAFT dispersion polymerisation reaction. As with the solution polymerisation, the overall rate of reaction was faster in flow than in batch, with high conversions (>90 %) obtained after 40 minutes compared to 60 minutes (Figure S6). Once again, we attribute this to the increased heat transfer in tubular flow reactors during the early stages of the reaction. The kinetic profile (Figure 4a) was also characteristic of RAFT aqueous dispersion polymerisation, with a rate enhancement at approximately 40 % conversion.[35] This enhancement is due to the self-assembly of the growing amphiphilic polymer chains into spherical particles; once these particles form monomer in solution migrates into the core of the particles generating a high local concentration of monomer which results in an increased rate of polymerisation. The ability to take samples over relatively short timescales resulted in much better resolution of this feature in the flow experiment. This again demonstrates that the technique is potentially powerful for future mechanistic studies. This could potentially enable improved accuracy during automated rate determination experiments. As was the case with the solution polymerisation, a linear increase in M_n with conversion (Figure 4b and c) and low molar mass dispersities were observed throughout the kinetic experiments (Figure S8).

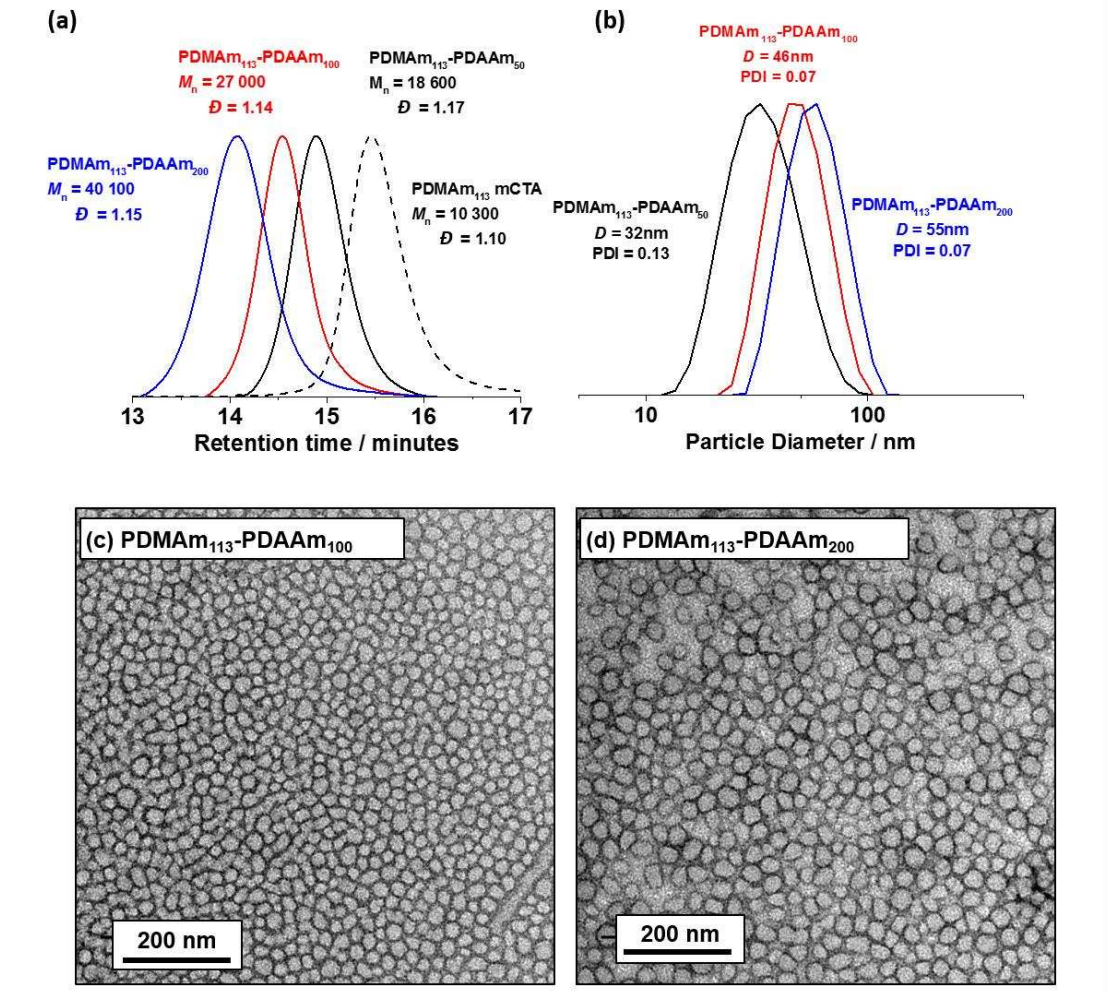

Figure 5. (a) GPC chromatograms and (b) DLS size distributions obtained for the chain extension of $PDMA_{113}$ with DAAm conducted using the continuous-flow reactor. (c) and (d) show TEM images obtained for $PDMAm_{113}$-$PDAAm_{100}$ and $PDMAm_{113}$-$PDAAm_{200}$ diblock copolymer spheres. For all reactions, total solids concentration of 10 % w/w and [CTA]:[Initiator] = 1:0.1.

Using the kinetic data acquired, a series of well-defined $PDMAm_{113}$-$PDAAm_X$ copolymers were synthesised employing the syringe pump and a 5 mL reactor coil with a residence time of 50 min. The resulting diblock copolymer dispersions were characterised using ^{1}H NMR, GPC and DLS (Table 1). NMR studies indicated near complete conversion was achieved in all cases while GPC confirmed systematic increase in molar mass in line with target DP of the PDAAm block. Furthermore, the molar mass distribution for each sample was mono-modal, while dispersities were all below 1.17 (Figure 5a). DLS indicated particles sizes of 32, 46 and 55 nm for PDAAm DPs of 50, 100 and 200 respectively. All samples had mono-modal particle size distributions (Figure 5b) with DLS reporting a PDI of 0.07 for DPs 100 and 200. A slightly broader PDI of 0.13 was reported for a PDAAm DP of 50, which is likely to do with the increased plasticisation of the micelle core due to the ingress of water. This DP is only slightly higher than that required for micellar nucleation during the synthesis (approx. DP 30) and therefore these particles are likely to comprise more loosely bound diblock copolymer chains. Transmission electron microscopy (TEM) studies confirmed the spherical morphology for DP 100 and 200 (Figure 5c and d), but no clear image was obtained for the DP of 50 (see supporting information Figure S9). This may be an artefact caused by the loosely bound nature of the block copolymer chains within the micelles.

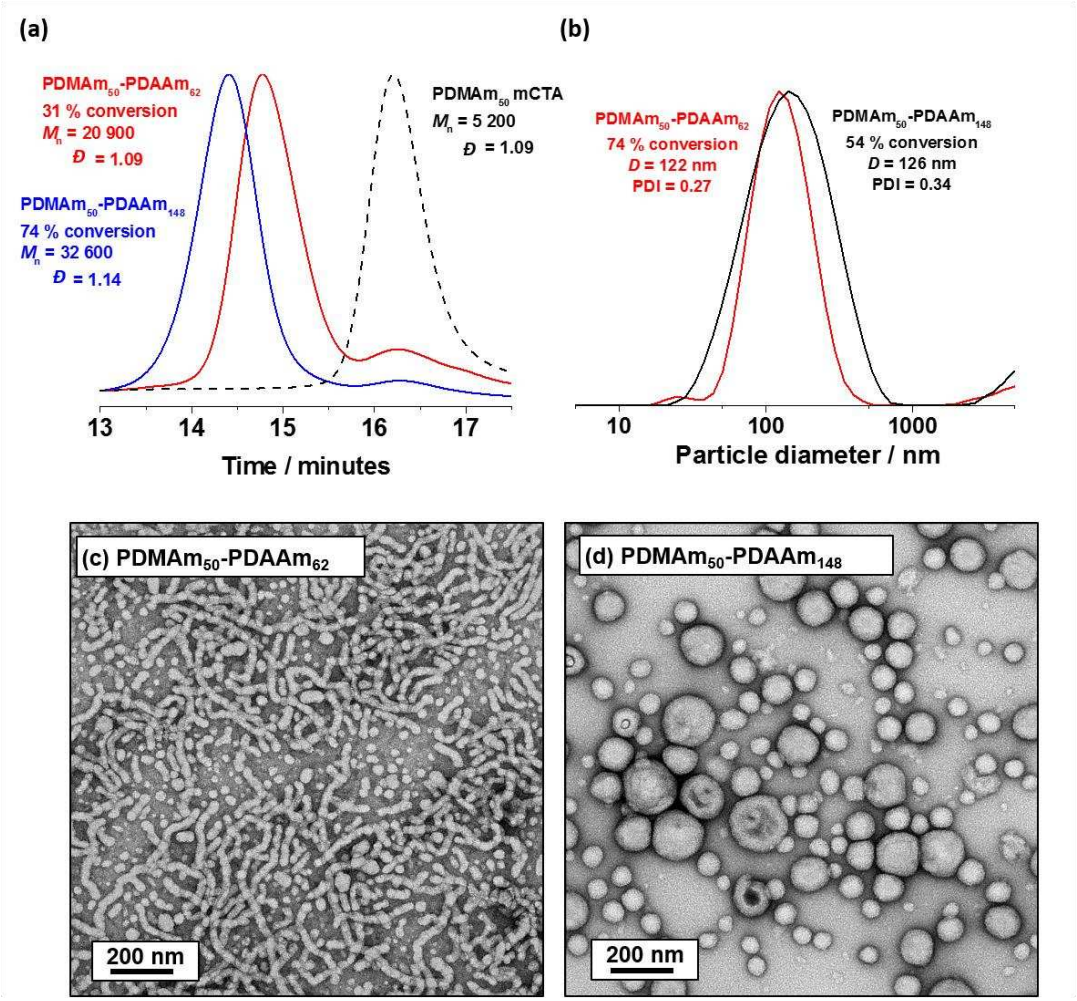

Figure 6. (a) GPC chromatograms and (b) DLS size distributions obtained for the chain extension of $PDMAm_{50}$ with DAAm conducted using the continuous-flow reactor. TEM images obtained for (c) $PDMAm_{50}$-$PDAAm_{62}$ worms and spheres and (d) $PDMAm_{50}$-$PDAAm_{148}$ vesicles and spheres. For both reactions, total solids concentration of 20 % w/w and [CTA]:[Initiator] = 1:0.1.

One of the attractive features of PISA is the ability to produce higher order block copolymer nano-objects. To investigate whether this was possible using our CF platform it was necessary to reduce the degree of polymerisation of the PDMAm macro-CTA and raise the total solids to 20 % w/w. According to the phase diagram reported by Byard et al., PDMAm DPs ≤ 58 can produce diblock copolymer worms or vesicles.[46] Hence, we prepared a $PDMAm_x$ macro-CTA with a DP of 50 and used it to mediate the CF RAFT dispersion polymerisation of DAAm at 20 % w/w. Two diblock copolymers were synthesised by employing two different residence times, for the same reaction solution which attained 31 % and 74 % conversion, equating to $PDMAm_{50}$-$PDAAm_{62}$ and $PDMAm_{50}$-$PDAAm_{148}$ respectively. A systematic increase in M_n with conversion from 20,900 to 32,600 g mol^{-1} was confirmed by GPC (see Figure 6a). This technique also confirmed low molar mass dispersities with low levels of macro-CTA contamination. We anticipate this macro-CTA contamination is in part due to some macro-CTA chains which have not yet initiated polymer chains combined with low levels of 'dead' chains, which can occur due to high conversion in macro-CTA syntheses. Nevertheless, these should not affect the self-assembly process. Broad and multimodal DLS distributions for the samples (Figure 6b) suggested the presence of non-spherical morphologies, and closer visual inspection indicated that some larger aggregates were present which may also account for the features corresponding to larger species in the multi-modal DLS traces. Nevertheless, TEM images obtained for the two samples (Figure 6c and d) indicated that the $PDMAm_{50}$-$PDAAm_{62}$ comprised a majority phase of block copolymer worms while the $PDMAm_{50}$-$PDAAm_{148}$ copolymer formed a majority phase of vesicles. A minor population of spherical particles was observed in both samples, but it should be noted that it has previously been reported that pure phases are difficult to obtain with this copolymer formulation.[46] It is also possible that excess monomer and the less well understood fluid mechanics add additional complications.

Final Copolymer Composition	Conv. [%]	M_n [g mol^{-1}]	$Đ$	Diameter [nm]	PDI	Morphology
	^{1}H NMR	DMF GPC		DLS		TEM
$PDMAm_{113}$-$PDAAm_{50}$	>99	18,600	1.17	32	0.13	S
$PDMAm_{113}$-$PDAAm_{100}$	>99	27,000	1.14	46	0.07	S
$PDMAm_{113}$-$PDAAm_{200}$	>99	40,100	1.15	55	0.07	S
$PDMAm_{50}$-$PDAAm_{62}$	31	20,900	1.09	126	0.34	W+S
$PDMAm_{50}$-$PDAAm_{148}$	74	32,600	1.15	122	0.27	V+S

Table 1. Details of the diblock copolymers prepared via continuous-flow RAFT aqueous dispersion polymerisation using a $PDMAm_{113}$ macro-CTA. Syntheses with $PDMAm_{113}$ macro-CTA were conducted at 10 % w/w solids, 70 °C and [CTA]:[ACVA] = 1:0.1. Syntheses with $PDMAm_{50}$ macro-CTA were conducted at 20 % w/w solids, 70 °C and [M]:[CTA]:[ACVA] = 200:1:0.1. Monomer conversion was determined by ^{1}H NMR spectroscopy in CD_3OD, M_n and $Đ$ were determined by DMF GPC vs. a series of near monodisperse poly (methyl methacrylate) standards, and all size measurements were determined by DLS. Sphere, worm and vesicle morphologies indicated by S, W and V respectively and judged by DLS and TEM. Composition calculated based on monomer conversion obtained from ^{1}H NMR spectroscopy.

Conclusions

This study has demonstrated for the first time, it is possible to conduct an all-aqueous synthesis of block copolymer spheres, worms and vesicles where both the macro-CTA and diblock copolymer are synthesised in continuous-flow reactors. Furthermore, a convenient method of conducting high-resolution transient kinetic studies gives close agreement with steady-state methods with the benefit of shorter timescales and reduced material consumption. Accelerated reaction rates in the flow reactors were observed, attributed to differing heat transfer rates early in the reaction: better heat transfer in flow increases radical flux which results in an overall faster polymerisation. The kinetic data was used to select conditions for scaling up the reaction using a modified reactor upgraded with HPLC pumps and a 20 mL reactor coil. This enabled a considerable increase in product output. This large batch of macro-CTA was successfully used to synthesise a series of $PDMAm_{113}$-$PDAAm_x$ diblock copolymers via CF RAFT dispersion polymerisation. Accelerated kinetics were again observed (vs. batch), high conversions, low molar mass dispersities and near complete blocking efficiencies were achieved. The resulting polymers underwent PISA to form spherical nanoparticles as judged by DLS and TEM. Finally, a shorter $PDMAm_{50}$ macro-CTA was successfully used at 20 % w/w to prepare both worms and vesicles by tailoring the residence time to achieve specific degrees of polymerisation of the PDAAm block. We believe the observations within this work have considerable implications with respect to process intensification and automation in the context of block copolymer synthesis.

Conflicts of Interest

There are no conflicts to declare.

Acknowledgements

We thank the EPSRC for providing a studentship for SP through the Doctoral Training Account and support for NW through an EPSRC New Investigator Award (EP/S000380/1), the University of Leeds for a University Academic Fellowships for NJW and NSH, and the Royal Society U.K. (RS Research Grant RSG\R1\180334). Ouassef Nahi is thanked for TEM analysis. We also thank the reviewers whose comments have considerably improved the quality of this manuscript.

References

1. D. E. Fitzpatrick, C. Battilocchio and S. V. Ley, *ACS Cent. Sci.*, 2016, **2**, 131-138.
2. S. G. Newman and K. F. Jensen, *Green Chem.*, 2013, **15**, 1456-1472.
3. R. M. Myers, D. E. Fitzpatrick, R. M. Turner and S. V. Ley, *Chem. Eur. J.*, 2014, **20**, 12348-12366.
4. J. J. Haven and T. Junkers, *Eur. J. Org. Chem.*, 2017, **2017**, 6474-6482.
5. N. Holmes, G. R. Akien, A. J. Blacker, R. L. Woodward, R. E. Meadows and R. A. Bourne, *React. Chem. Eng.,* 2016, **1**, 366-371.
6. M. Rubens, J. H. Vrijsen, J. Laun and T. Junkers, *Angew. Chem. Int. Ed.*, 2018, **0**.
7. C. M. Bates and F. S. Bates, *Macromolecules*, 2017, **50**, 3-22.
8. J.-S. Wang and K. Matyjaszewski, *J. Am. Chem. Soc.*, 1995, **117**, 5614-5615.
9. 1984.
10. J. Chiefari, Y. K. Chong, F. Ercole, J. Krstina, J. Jeffery, T. P. T. Le, R. T. A. Mayadunne, G. F. Meijs, C. L. Moad, G. Moad, E. Rizzardo and S. H. Thang, *Macromolecules*, 1998, **31**, 5559-5562.
11. G. Moad, E. Rizzardo and S. H. Thang, *Aust. J. Chem.* 2012, **65**, 985-1076.
12. X. Li, E. Mastan, W.-J. Wang, B.-G. Li and S. Zhu, *React. Chem. & Eng.*, 2016, **1**, 23-59.
13. T. Junkers and R. Hoogenboom, *Eur. Polym. J.*, 2016, **80**, 175-176.
14. Y. Shen and S. Zhu, *AlChE J.*, 2002, **48**, 2609-2619.
15. Y. Shen, S. Zhu and R. Pelton, *Macromol. Rapid Commun.*, 2000, **21**, 956-959.

16. C. H. Hornung, C. Guerrero-Sanchez, M. Brasholz, S. Saubern, J. Chiefari, G. Moad, E. Rizzardo and S. H. Thang, *Org. Process Res. Dev.*, 2011, **15**, 593-601.
17. N. Micic, A. Young, J. Rosselgong and C. Hornung, *Processes*, 2014, **2**, 58.
18. C. Diehl, P. Laurino, N. Azzouz and P. H. Seeberger, *Macromolecules*, 2010, **43**, 10311-10314.
19. M. Chen and J. A. Johnson, *Chem. Commun.*, 2015, **51**, 6742-6745.
20. J. Gardiner, C. H. Hornung, J. Tsanaktsidis and D. Guthrie, *Eur. Polym. J.*, 2016, **80**, 200-207.
21. T. Junkers and B. Wenn, *React. Chem. Eng*, 2016, **1**, 60-64.
22. N. Corrigan, D. Rosli, J. W. J. Jones, J. T. Xu and C. Boyer, *Macromolecules*, 2016, **49**, 6779-6789.
23. A. Kuroki, I. Martinez-Botella, C. H. Hornung, L. Martin, E. G. L. Williams, K. E. S. Locock, M. Hartlieb and S. Perrier, *Polym. Chem.*, 2017, **8**, 3249-3254.
24. M. Rubens, P. Latsrisaeng and T. Junkers, *Polymer Chemistry*, 2017, **8**, 6496-6505.
25. C. H. Hornung, A. Postma, S. Saubern and J. Chiefari, *Macromol React Eng,* 2012, **6**, 246-251.
26. J. Vandenbergh and T. Junkers, *Polym. Chem.*, 2012, **3**, 2739-2742.
27. C. H. Hornung, K. von Känel, I. Martinez-Botella, M. Espiritu, X. Nguyen, A. Postma, S. Saubern, J. Chiefari and S. H. Thang, *Macromolecules*, 2014, **47**, 8203-8213.
28. C. H. Hornung, X. Nguyen, G. Dumsday and S. Saubern, *Macromol. React. Eng.*, 2012, **6**, 458-466.
29. S. Saubern, X. Nguyen, V. Nguyen, J. Gardiner, J. Tsanaktsidis and J. Chiefari, *Macromol. React. Eng.*, 2017, **11**, 1600065.
30. L. Xiang, W.-J. Wang, B.-G. Li and S. Zhu, *Macromolecular Reaction Engineering*, 2017, **11**, 1700023.
31. N. Corrigan, R. Manahan, Z. T. Lew, J. Yeow, J. Xu and C. Boyer, *Macromolecules*, 2018, DOI: 10.1021/acs.macromol.8b00673.
32. N. Corrigan, A. Almasri, W. Taillades, J. Xu and C. Boyer, *Macromolecules*, 2017, **50**, 8438-8448.
33. F. Bally, C. A. Serra, C. Brochon and G. Hadziioannou, *Macromol. Rapid Commun.*, 2011, **32**, 1820-1825.
34. B. Charleux, G. Delaittre, J. Rieger and F. D'Agosto, *Macromolecules*, 2012, **45**, 6753-6765.
35. N. J. Warren and S. P. Armes, *J. Am. Chem. Soc.*, 2014, **136**, 10174-10185.
36. S. L. Canning, G. N. Smith and S. P. Armes, *Macromolecules*, 2016, **49**, 1985-2001.
37. N. J. Warren, O. O. Mykhaylyk, A. J. Ryan, M. Williams, T. Doussineau, P. Dugourd, R. Antoine, G. Portale and S. P. Armes, *J Am Chem Soc*, 2015, **137**, 1929-1937.
38. N. J. Warren, M. J. Derry, O. O. Mykhaylyk, J. R. Lovett, L. P. D. Ratcliffe, V. Ladmiral, A. Blanazs, L. A. Fielding and S. P. Armes, *Macromolecules*, 2018 **51** 8357-8371..
39. Z. Li, W. Chen, Z. Zhang, L. Zhang, Z. Cheng and X. Zhu, *Polym. Chem.*, 2015, **6**, 1937-1943.
40. J. Peng, C. Tian, L. Zhang, Z. Cheng and X. Zhu, *Polym. Chem.*, 2017, **8**, 1495-1506.
41. N. Zaquen, J. Yeow, T. Junkers, C. Boyer and P. B. Zetterlund, *Macromolecules*, 2018, **51**, 5165-5172.
42. N. Chan, S. Boutti, M. F. Cunningham and R. A. Hutchinson, *Macromol. React. Eng.*, 2009, **3**, 222-231.
43. J. S. Moore and K. F. Jensen, *Angew. Chem. Int. Ed.*, 2014, **53**, 470-473.
44. C. A. Hone, N. Holmes, G. R. Akien, R. A. Bourne and F. L. Muller, *React Chem Eng.*, 2017, **2**, 103-108.
45. K. C. Aroh and K. F. Jensen, *React Chem Eng.*, 2018, **3**, 94-101.
46. S. J. Byard, M. Williams, B. E. McKenzie, A. Blanazs and S. P. Armes, *Macromolecules*, 2017, **50**, 1482-1493.
47. W. Zhou, Q. Qu, Y. Xu and Z. An, *ACS Macro Letters*, 2015, **4**, 495-499.
48. O. J. Deane, J. R. Lovett, O. M. Musa, A. Fernyhough and S. P. Armes, *Macromolecules*, 2018, **51**, 7756-7766.
49. G. Gody, R. Barbey, M. Danial and S. Perrier, *Polym. Chem.*, 2015, **6**, 1502-1511.
50. T. Junkers, *Macromol. Chem. and Phys.*, 2017, **218**.
51. R. W. Carr and R. V. Poirier, *J. Phys. Chem.* , 1971, **75**, 1593-1601.